Frataxin deficiency induces schwann cell inflammation and death

Chunye Lu, Robert Schoenfeld, Yuxi Shan, Cindy Tsai, Bruce Hammock, Gino Cortopassi

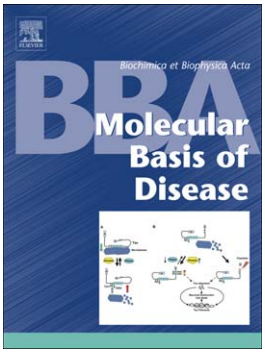

Frataxin deficiency induces schwann cell inflammation and death

Chunye Lu, Robert Schoenfeld, Yuxi Shan, Cindy Tsai, Bruce Hammock, Gino Cortopassi

PII: S0925-4439(09)00164-1
DOI: doi: 10.1016/j.bbadis.2009.07.011
Reference: BBADIS 62984

To appear in: *BBA - Molecular Basis of Disease*

Received date: 11 September 2008
Revised date: 18 June 2009
Accepted date: 27 July 2009

Please cite this article as: Chunye Lu, Robert Schoenfeld, Yuxi Shan, Cindy Tsai, Bruce Hammock, Gino Cortopassi, Frataxin deficiency induces schwann cell inflammation and death, *BBA - Molecular Basis of Disease* (2009), doi: 10.1016/j.bbadis.2009.07.011

Frataxin Deficiency Induces Schwann Cell Inflammation and Death

Chunye Lu, Robert Schoenfeld, Yuxi Shan, Cindy Tsai, Bruce Hammock and Gino Cortopassi*

Department of Molecular Biosciences, University of California, Davis, California, 95616

*Corresponding author. VM: Dept. of Molecular Biosciences, 1311 Haring Hall, Davis, CA 95616.
Tel. 5307549665;
Fax. 5307549342;
Email: gcortopassi@ucdavis.edu

Keywords: Friedreich's ataxia (FRDA), dorsal root ganglia (DRG) neuron, Schwann cells, Inflammatory response, siRNA, frataxin

Summary

Mutations in the frataxin gene cause dorsal root ganglion demyelination and neurodegeneration, which leads to Friedreich's ataxia. However the consequences of frataxin depletion have not been measured in dorsal root ganglia or Schwann cells. We knocked down frataxin in several neural cell lines, including two dorsal root ganglia neural lines, 2 neuronal lines, a human oligodendroglial line (HOG) and multiple Schwann cell lines and measured cell death and proliferation. Only Schwann cells demonstrated a significant decrease in viability. In addition to the death of Schwann cells, frataxin decreased proliferation in Schwann, oligodendroglia, and slightly in one neural cell line. Thus the most severe effects of frataxin-deficiency were on Schwann cells, which enwrap dorsal root ganglia neurons. Microarray of frataxin-deficient Schwann cells demonstrated strong activations of inflammatory and cell death genes including interleukin-6 and Tumor Necrosis Factor which were confirmed at the mRNA and protein levels. Frataxin knockdown in Schwann cells also specifically induced inflammatory arachidonate metabolites. Anti-inflammatory and anti-apoptotic drugs significantly rescued frataxin-dependent Schwann cell toxicity. Thus, frataxin deficiency triggers inflammatory changes and death of Schwann cells that is inhibitable by inflammatory and anti-apoptotic drugs.

Introduction

Friedreich's ataxia (FRDA) is a neurodegenerative and demyelinating disorder that affects primarily the dorsal root ganglia, the posterior column, spinocerebellar pathways and the pyramidal tracts of the spinal cord[1-6]. The essential features of the neuropathology of FRDA is a distal length-related axonal degeneration that affects the corticospinal and dorsal spinocerebellar tracts and the dorsal columns, and the degeneration extends towards the cell bodies in a “dying back” manner and eventually leads to loss of dorsal root ganglion neurons[7].The non-neurological aspects of the phenotype include cardiac hypertrophy and insulin insensitivity [8, 9]. FRDA is caused by the mutations in the autosomal frataxin gene that lead to decreased frataxin protein. Data from human studies and genetic models suggest that iron sulfur protein defects and oxidative stress are the primary molecular consequences of frataxin deficiency [10, 11]. However, it is still unclear how these biochemical consequences of frataxin deficiency result in the clinical manifestations of FRDA including neurodegeneration and demyelination.

Previously, the consequences of frataxin depletion in embryonal P19 stem cells, some of which differentiate into diverse neural cell types have been studied using antisense technology, and increased death and decreased differentiation were observed[12]. However in Friedreich's ataxia there is a specific demyelination and degeneration mainly of dorsal root ganglia neurons, which are quite different from the neurons produced by differentiation of p19. So, to study the specific consequences of frataxin depletion in the DRG, neural and glial cellular environments, we knocked down frataxin in DRG neural (rat DRG/mouse

neuroblastoma hybrid, ND7/23, and rat DRG-derived neuronal cell line, 50B11), neuronal (rat PC12 and human neuronal cell line NT2), human oligodendroglial (HOG) and Schwann (T265, ST88 and STS26T) cells. We observed strong and selective inflammatory toxicity of frataxin deficiency to Schwann cells which seemed interesting, because the axons of DRG neurons are enwrapped by Schwann cells, and because Schwann cells have previously been described to undergo a conversion to an inflammatory phenotype[13-17]. Frataxin deficiency also inhibited cell proliferation in HOG cells, Schwann cells and NT2 cells, but not in the 2 DRG lines and PC12. Thus by this secondary criterion of proliferation, support cells were more sensitive to frataxin-deficiency than DRG neurons.

Materials and methods

Cell culture

Human Schwann cell lines (T265, STS26T, ST88), human oligodendroglioma (HOG) cell line and the DRG cell line (ND7/23, rat DRG/mouse neuroblastoma hybrid) were maintained in DMEM, supplemented with 10% FBS, 1% pen/strep and 2mM glutamine. Rat PC12 cells were grown in RPMI 1640 medium containing 10% FBS, 1% pen/strep and 2mM glutamine. Human NT2 cells were maintained in DMEM/F12 medium, supplemented with 10% FBS, 1% pen/strep, 2mM glutamine, 50 µg/ml uridine and 1 µM sodium pyruvate. The rat DRG-derived neuronal cell line, 50B11, was maintained in Neurobasal medium supplemented with 10% FBS, 2% B-27 Supplement (Invitrogen), 0.1% glucose, 0.5 mM glutamine and 5 µg/ml blasticidin (Invitrogen). Cells were passaged every 3-4 days.

Cell cycle analysis

About 0.7 million cells were harvested and washed with PBS. The cell pellet was resuspended in 0.5 ml PBS, and fixed in 70% ethanol at -20ºC overnight. The ethanol-suspended cells were centrifuged and washed with PBS. The cell pellet was suspended in 0.5 ml staining buffer (0.02mg/ml PI, 0.1% (v/v) Triton X-100 in PBS, 0.2mg/ml RNase A) and incubated 15 min at 37 ºC then analyzed by flow cytometry (Becton Dickinson FACScan) at the UC Davis Optical Biology Shared Resource. Triplicate wells were used for each experiment.

Cell growth assay

Trypan Blue exclusion Assay: Reverse transfection was performed with 0.3 million cells per well in 6-well plates. At different time points (range from 1 to 3 days) after the transfection cells were harvested and counted by vi-cell (Beckman coulter). For Schwann cells and HOG cells, the floating and attached cells were harvested and counted separately. The experiments were repeated at least 3 times using triplicate wells for each treatment.

Apoptosis assay -- Alexa Fluor 488 Annexin V and PI double staining

Alexa Fluor 488 -labeled annexin-V and PI double staining assay was used to examine the frataxin deficiency-dependent apoptosis using the Vybrant apoptosis assay kit #2 (Invitrogen). Briefly, cells were harvested and washed in cold PBS. The cell pellet was resuspended in 100 µl of 1×annexin- binding buffer prior to the incubation with Annexin-V/PI for 15 min at room temperature in the dark. After the incubation, 400 µl of 1×annexin- binding buffer was added and keep the samples on ice for analysis on the flow cytometer. Thirty thousand cells were analyzed per

sample. Apoptotic cells were defined as FITC+/PI− cells. Triplicate wells were used for each experiment.

Microarray

Microarray sample preparation and data analysis was performed as previously described [18].

Oxylipin profiling assay

The same number of cells was plated on each culture dishes for siRNA transfection. 3 days post-transfection, media were collected and spinned to removed cells and debris. The supernatants were frozen until the oxylipin profiling assay. The oxylipins were quantified by HPLC/MS/MS using internal standard methods [19].

Quantitative PCR

Quantitative PCR was performed as previously described using the Lightcycler 1.2 or Lightcycler 480 (Roche). The sequences of each primer pair for each gene are shown in Table 3.

Cytokine assay

Cytokine protein expressions were assayed in cell culture supernatants using Pierce's SearchLight™ multiplex sandwich ELISA analysis service or using luminex assay service from Department of Pathology and Laboratory Medicine's Clinical Proteomics Core at UC Davis. Briefly, cell culture medium was collected and centrifuged to remove cells or debris. The supernatants were frozen and shipped on dry ice. The cytokine concentrations were normalized to per ml cell culture supernatant per million cells.

siRNA transfection

Reverse transfection involving simultaneously transfecting and plating cells was performed using lipofectamine 2000 according to the manufacture protocol (Invitrogen). Briefly, transfection mix including siRNA (30nM final concentration, except 40nM for ND7/23) and transfection reagent was made and added to the wells in 6-well plates. The cells were harvested by trypsinization and about 0.3 million cells was plated in the wells with the transfection mix. siRNAs used in the study includes: human frataxin siRNA described previously[20], AAC GUG GCC UCA ACC AGA UUU, and scrambled siRNA, CAG UCG CGU UUG CGA CUG GdTdT, human frataxin siRNA (ON-TARGETplus duplex #J-006691-07) and non-targeting siRNA (D-001810-0X), Rat frataxin siRNA (ON-TARGETplus SMARTpool, L-104901-01), mouse frataxin siRNA (ON-TARGETplus SMARTpool, #L-045500-00), and control siRNA (Non-Targeting Pool, #D-001810-10) from Dharmacon.

Western blot analysis

Cells were lysed in lysis buffer (20mM Tris pH7.5, 150 mM NaCl, 1% NP-40, 0.5% Sodium Deoxycholate, 1mM EDTA, 0.1% SDS) containing protease inhibitor cocktail and phosphatase inhibitor cocktail from Sigma (if the lysate was used for detect phophorylated proteins) at 4 ºC for 30 min. The supernatant was recovered by centrifugation. Equal amount of lysates (40ug) were used for immunoblotting. Protein concentration was assayed by the Bradford protein assay system (Bio-rad). Western blotting was performed as described [20] or using the Odyssey Infrared Imaging System (Li-Cor). Primary antibodies used to detecting phosphorylated p38, JNK, p44/42 and total p38, JNK, p44/42 are from Cell Signalling Technology. Primary frataxin antibody was described by Tan et al [21].

Results

Frataxin knockdown is selectively toxic to Schwann cells

To evaluate the effects of frataxin deficiency on target cell types, we knocked down frataxin by siRNA in multiple neuronal and glial cell lines. Frataxin levels were measured by quantitative PCR 3 days after the siRNA transfection, and residual frataxin was 20% or less of controls, similar to levels observed in FRDA patients (Fig. 1A). Many floating cells were only observed in frataxin-deficient Schwann cells, consistent with a toxic effect of frataxin-deficiency, so the floating and the adherent cells were collected and counted separately, and viability and cell count were determined using the Beckman Coulter Vi-Cell cell counter. The total cell number (floating + adherent) was significantly reduced at day 3 in frataxin-deficient Schwann cells, HOG cells and NT2 cells, but not in the DRG lines and PC12 cells (Fig. 1D). These results suggested that frataxin-deficiency either decreased cell proliferation and/or increased cell death of the former 3 cell lines. For the HOG cells, there was no significant decrease in viability, and only a small increase in floating cells (Fig. 1B and C), indicating that the decrease in cell number is the result of decreased cell proliferation. Similar to the HOG cells, frataxin depletion inhibited the cell proliferation without affecting the cell viability in NT2 cells (Fig. 1 B and D). By contrast, frataxin deficiency in Schwann cells caused a significant decrease in cell viability and a five-fold increase in floating cells (Fig. 1B and C). Furthermore, we observed a similar frataxin-dependent decrease in cell viability and increased floating cells in two other Schwann cell lines (ST-88 and STS26T) (S.Fig.1A-D). We

did not observe decreased viability nor decreased cell proliferation in the 2 DRG lines and PC12 cells.

Inhibition of cell cycle precedes apoptotic death in frataxin-deficient Schwann cells.

To further dissect the cellular toxicity caused by frataxin deficiency in Schwann cells, we carried out a time course study to investigate whether the frataxin-dependent inhibition of cell proliferation and decreased viability could be separated in time. At 24 hours, frataxin protein shows very small decrease by siRNA (an average of 28%) by densitometry analysis of 3 indepedent experiments, with an greater decrease (an average of about 50%) observed at day2 and greater than 70% at day3 (Fig.2E). Consistent with these observations, the total cell number was minimally decreased, and no significant changes in floating cell number or viability were observed at day1 (Fig.2A-C). Thus, a defect in cell growth is significantly perceptible before a rise in cell death. At 48 hours, cell number decreased by 300,000 with respect to controls (Fig. 2A), with a significant increase in floating cell number and significant decrease in cell viability (Fig. 2B and C). The most prominent effects on total cell number, floating cell number and viability were observed at day3 (Fig. 2 A, B, C), when frataxin protein is down to less than 30% of control. Thus, frataxin deficiency causes an early decrease in cell proliferation followed by an increase in death in Schwann cells. Further, flow cytometry analysis with frataxin-deficient Schwann cells at day 3 demonstrated that a significantly increased number of apoptotic cells and necrotic cells were observed (table 1). By contrast, no significant increase in apoptotic cells was found in frataxin-deficient

HOG cells (table 1). Thus, frataxin-deficiency triggers apoptotic death of Schwann cells, but not oligodendroglial cells. This suggests that it is not the myelinating phenotype per se that sensitizes cells to frataxin deficiency but something more Schwann-cell specific.

Frataxin deficiency causes an inhibition of cell cycle progression in Schwann and oligodendroglial cells

To further characterize the frataxin-dependent inhibition of cell proliferation, cell cycle analysis was performed by flow cytometry analysis at day 3. For both Schwann cells and HOG cells, frataxin depletion decreased the fraction of cells in S phase by about half, increased the fraction of cells in G_2M by two-fold, and increased the fraction of cells in G_0G_1 by a few percent (Fig. 3). Thus, frataxin depletion inhibits mitosis, i.e., blocks the transition from G_2 to M phase. This block in mitosis was confirmed by the observation of an increase in cell size in frataxin-inhibited cells (Fig. 4). Furthermore peaks of cell population with DNA content greater than 4X increase in the frataxin-deficient Schwann cells, consistent with a mitotic block (S.Fig.2).

Frataxin knockdown causes a phenotypic change in Schwann cells

Frataxin-deficient Schwann cells underwent a major morphological change at 2 days post-knockdown. Fig. 4A shows the typical Schwann cell morphology, i.e. elongated spindle-shaped and bipolar morphology. By contrast, after 2 days of frataxin knockdown, Schwann cells became more round, with large, obvious cytoplasmic vesicular granules. More profound morphological changes were

observed at day3 (Fig. 4B). Two other Schwann cell lines (ST88 and STS26T) showed similar morphological changes (S.Fig.1E-H).

Microarray of frataxin-deficient cells shows a selective activation of genes involved in inflammation and death

We microarrayed the Schwann cells in an attempt to identify the pathways activated by frataxin-deficiency. Cells were collected 3 days after transfecting siFxn or scrambled siRNA. mRNA was isolated with RNeasy kit (Qiagen). Microarray sample preparation and data analysis were performed as described [20]. We carried out microarray on biological duplicates (2 scr vs. 2 siFxn). The top 500 up-regulated, and top 500 down-regulated genes (S.Table.1) were analyzed by Onto-Express program to identify the most affected biological processes from a given gene list. Table 2 shows that inflammation and apoptosis are most significantly -upregulated pathways in the frataxin-depletion Schwann cells, and that cell cycle is a top-inhibited pathway. The microarray results supported the cellular results, i.e. an observation of increased cell death and decreased proliferation. By contrast, we did not observe a strong induction of inflammatory and apoptotic genes in frataxin-deficient HOG cells (data not shown) by microarray, indicating that the induction of inflammatory and apoptotic genes is specific to Schwann cells, even though both of these cell types are myelinating. Inflammatory and death genes strongly induced in the microarray data of frataxin-deficient Schwann cells include interleukin 1 beta (11X), interleukin 1 alpha (9X), interleukin 6 (7X), NFkB1 (3X), NFkB2 (3X), Tumor Necrosis factor (4X), phospholipase A2G4C (PLA2G4C, 3 X), phospholipase A2G6

(PLA2G6, 2 X), phospholipase A2G7 (PLA2G7, 2 X), prostaglandin-endoperoxide synthase 2 (3 X), prostaglandin E synthase (2 X), and several chemokine genes. Interestingly, our previous microarray data of FRDA patients lymphoblasts also showed a significant induction of several inflammatory genes, including caspase 1, TNF subfamily 2 (also named TNF), IL-6, interferon-inducible p78 and TNF alpha induced p6 [20].

Inflammatory genes are induced by frataxin deficiency in Schwann cells at the transcript and protein levels.

To confirm the transcriptional inductions of inflammatory transcripts, quantitative RT-PCR was performed on several genes: TNF, IL6, IL1B, NFkB1 and NFkB2 in 3 Schwann cell lines and the results are shown in Fig. 5A and S.Fig.1I-J. The transcripts of TNF, IL6, IL1B increased by more than 5-fold. Multiplex sandwich ELISAs were used to measure the protein levels of several cytokines: TNF, IL6, CSF3, IL1A, IL1B, GMCSF, IL8 and IFN-alpha. Fig. 6 shows that 7 cytokine protein levels were significantly increased, consistent with the induction at the mRNA level by microarray. IL6 protein was observed to have a high basal expression and be induced by about 4 fold upon frataxin deficiency (Fig. 6).

To assess the time course of cytokine induction and cell death, IL6 levels were measured 1-3 days after frataxin knockdown. Fig. 2D shows that IL6 increased by 40% 1 day post-knockdown, a time at which there was no significant increase in cell death. A greater increase was observed at 2 and 3 days. The time course study

suggests that cytokine induction preceded cell death in frataxin-deficient Schwann cells.

To insure that all effects we observed in Schwann cells were truly frataxin-dependent rather than off-target effects of the siRNA, we repeated our experiments with another siRNA validated to have minimal non-specific effects (Dharmacon), We observed similar cellular effects: morphological change, decreased viability and proliferation and induced cytokine expressions (S.Fig.3).

Inflammatory arachidonate metabolites increase in frataxin-deficient Schwann Cells

Our microarray data demonstrates an upregulation of multiple forms of PLA2, and PLA2 activity results in the hydrolysis of membrane phospholipids and the release of arachidonic acid, which is a precursor of eicosanoids. Thus we measured oxidized lipids that are mediators of inflammation (lipid-derived eicosanoids, including prostaglandins, thromboxanes and leukotrienes) using HPLC coupled with mass spectrometry. Cell culture medium was collected at day 3 post-knockdown and the metabolite concentrations were measured. Student's *t* tests were used to determine the statistical significance of the results for each analyte. We measured 40 arachidonic acid derivatives catalyzed by cyclooxygenase (COX) (prostaglandins) and lipoxygenases (LOX) (leukotrienes), as well as cytochrome P450 enzymes (Fig.7A). After application of a false discovery rate correction ($q = 0.05$), significant induction of 15 metabolites from COX pathway, LOX pathway and P450 epoxygenase–sEH metabolic pathway were observed with $p < 0.02$ (Fig.7B and C). Of the three major branches, the LOX and COX pathway metabolites were most strongly induced.

Anti-inflammatory and anti-apoptotic drugs rescue Schwann cells from death

We tested several categories of drugs to see if we could rescue cell death in frataxin-deficient Schwann cells, including iron chelators (DFO, L1), antioxidants (NAC, BHA, BHT, NDGA, MntBAP) and anti-apoptotic agents (Q-VD-OPH, BAF, ZVAD). In addition, several anti-inflammatory agents were tested. These compounds included: 1, cytokine neutralizing antibodies: anti-IL6, anti-IL1B and anti-TNF; 2, NFkB inhibitor: salicylate; 3, several phospholipase 2 inhibitors: Quinacrine, arachidonyltrifluoromethyl ketone, ATFK, Methyl Arachidonyl Fluorophosphonate MAFP, Bromoenol lactone (BEL) and Palmitoyl trifluoromethyl ketone (PACOCF3); 4, several lipoxygenase inhibitors: MK886, COX-2 inhibitor III and indomethacin; and 5, the anti-inflammatories dexamethasone (DEX), SB203580 and SKF86002. Several concentrations of each compound were tested. The rescue compounds were added 24 hours after the siRNA transfection, and were incubated with the cells for another 48 hours. Afterwards, the cells were collected for cell counting assay (floating cell number, total cell number and viability) by vi-cell (Beckman coulter) or/and double staining with PI and annexin V followed by flow cytometry analysis. None of the drugs described above provided rescue except the anti-apoptotic Q-VD-OPH (5μM), and the anti-inflammatories dexamethasone (250nM), SB203580 (20μM) and SKF86002 (10μM).

The potent anti-apoptotic drug Q-VD-OPH was found to significantly decrease the floating cells and increase the cell viability by Vi-cell analysis (data not shown). The partial rescue from the cell death was also confirmed by flow cytometry analysis

(Table 1). The portion of dead cells (UR+LR, i.e., necrotic cells+ apoptotic cells) was observed to increase upon frataxin deficiency compared to the control, and the Q-VD-OPH treatment decreased the portion of dead cell from about 52% to about 25%.

Among several types of anti-inflammatory drugs tested, only dexamethasone, SB203580 and SKF86002 (2 specific inhibitors of p38 MAP kinase) partially rescued the death of frataxin-deficient Schwann cells. Both dexamethasone and SB203580 significantly decreased the number of floating cells and increased cell viability (Fig.8). Cytokine protein analysis revealed that dexamethasone treatment significantly decreased IL6 by 3-fold, and also significantly decreased TNF-alpha levels and IL1alpha levels (Fig.9). SB203580 significantly decreased mean IL1a levels and IL6 levels, albeit not significantly. SKF86002, another anti-inflammatory inhibitor of p38 MAP kinase, showed a similar level of rescue as SB203580 (data not shown).

We further investigated the phosphorylation of mitogen-activated protein (MAP) kinases by western blot. The results show that mean phosphorylated p38 MAP kinase was increased at day 3, however the increase was not significant. There was no increase in the phosphorylation of two other stress-related MAP kinases, c-Jun N-terminal kinases (JNKs) and p42/ p44 MAP Kinase (Erk1 and Erk2) (Fig. 10).

Although Q-VD-OPH rescued death of frataxin-deficient Schwann cells, it did not reduce TNF and IL6 protein levels (Fig.9). This is consistent with the time course study (Fig.2) and the mechanistic view that frataxin deficiency causes cytokine induction and then cell death. Thus, anti-inflammatories inhibit cytokine production and cell death, whereas anti-apoptotics inhibit only death but not cytokine production.

Discussion

Frataxin-deficiency inhibits proliferation in multiple neural cell types.

The mechanisms responsible for the demyelination and degeneration of dorsal root ganglion neurons in Friedreich's ataxia are poorly understood. Here we investigated the effects of frataxin deficiency in several neural cell lines, including PC12, DRG neurons, NT2, HOG cells and Schwann cells. Frataxin-deficiency neither inhibited the growth nor induced death of the DRG neural cell lines. However, frataxin deficiency inhibited the proliferation of Schwann cells and HOG cells, and to a lesser extent, NT2 neural cells.

The inhibition of the cell cycle depletes S phase cells and increases G_2M cells

Frataxin-deficiency inhibited cell cycle progression in Schwann cells, HOG cells and NT2 cells, but only caused death in Schwann cells. Non-synchronized cell cycle analysis demonstrated that cells were mainly blocked in mitosis, and subsequently there were a 2-fold increase in the fraction of cells in G_2M and increased cell size was observed under microscope. Consistent with these observations, microarray of the frataxin-deficient cells demonstrated inhibition of mitotic transcripts.

Frataxin-deficiency induces a morphological change and death uniquely in Schwann cells

Frataxin-deficiency only induced significant cell death in Schwann cells, and not the closely-related oligodendroglial HOG cells, nor DRG neurons, PC12 or NT2 neurons, suggesting a cell-type specific basis for this toxicity. Also, uniquely in

Schwann cells frataxin-deficiency induced profound morphological changes that were unlike apoptosis, and more like the induction of a phagocytic response. This transition to an inflammatory/phagocytic response has been previously noted in a large body of studies with Schwann cells[13, 16, 17, 22-25].

Induction of inflammatory and apoptotic genes precedes Schwann cell death

We observed that frataxin deficiency selectively and significantly induced inflammatory and cell death transcripts in Schwann cells by microarray, and that these increases were confirmed by QRTPCR and multiplex protein assay. We further showed the cellular toxicity could be partially rescued by the anti-inflammatory drugs SB203580 and SKF86002 and dexamethasone, and by the anti-apoptotic drug Q-VD-OPH. However, drugs from the antioxidant and iron-chelation classes had no beneficial effect on the frataxin-deficient Schwann cells.

It is now widely accepted that inflammation contributes to the pathogenesis of many neurodegenerative diseases of both inflammatory and primarily non-inflammatory origin, including Alzheimer's disease (AD)[26, 27], Parkinson's disease (PD) [28], Huntington's disease[29], Multiple sclerosis[30], Amyotrophic lateral sclerosis[31] and Wallerian degeneration[32], and is referred to as neuroinflammation. Neuroinflammation is characterized by activated neuroglial cells and the secretion of inflammatory mediators, among which, cytokines are thought to be the key players. In the peripheral nervous system (PNS), Schwann cells serve as partially immune-competent cells, capable of producing a variety of proinflammatory cytokines including IL1, IL6 and TNF, and other proinflammatory mediators such as

prostaglandin E2, thromboxane A2 and leukotriene C4[22, 33-36]. Here we demonstrated a strong inflammatory response upon frataxin deficiency in cultured human Schwann cell lines, including the secretion of multiples cytokines and other inflammatory mediators, e.g., metabolites of arachidonic acid. Transcription factors, nuclear factor-kappa B (NFkB1 and 2), were also upregulated, whose activity has been implicated in regulation of the innate inflammatory response including AD, i.e., upregulation of NFkB increase IL-1, IL6 and TNF-α levels [37, 38]. The arachidonate pathway has been shown to play a critical role in the production of potent inflammogens [39] and in neurodegenerative diseases including AD (for review, see: [40]). Here we demonstrate increased arachidonic acid derivatives catalyzed by COX, LOX, and P450 pathways in frataxin-deficient Schwann cells. A further study of arachidonic acid derivatives in FRDA patients is needed. Free radical generation and lipid peroxidation have been thought to play a significant role in FRDA. Upregulation of proinflammatory PLA2 and the subsequent release of lipid-derived eicosanoids may be one of the factors that are responsible for free radical generation and lipid peroxidation in FRDA.

Schwann cells are the myelinating cells of dorsal root ganglion neurons, and are thus in intimate physical contact with them. Thus we speculate that inflammatory cytokines produced by frataxin-deficient Schwann cells may contribute to DRG neuron toxicity. In Friedreich's ataxia patients, microscopic examinations of autopsied heart samples have revealed evidences of myocarditis with leukocyte infiltrations [41-43], suggesting that inflammation may play a role in the progressive cardiomyopathy in FRDA.

Consistent with the results in Schwann cells, we had previously demonstrated that frataxin-deficient lymphoblasts from Friedreich's patients overexpress multiple inflammatory transcripts including IL-6 and TNF, and that these inflammatory changes were rescued by frataxin transfection[20]. In Schwann cells, IL6 showed a very high basal expression and a significant induction of about 4 fold at the protein level. Therefore we assume that IL6 functions as a very important proinflammatory mediator secreted by Schwann cells. Inflammation can be induced by iron accumulation and oxidative stress[44, 45], both of which have been shown to be the consequences of frataxin deficiency.

Summary and Prospects

In this study we demonstrated that frataxin deficiency causes the inhibition of cell proliferation in several neuroglial cells including Schwann, HOG and NT2 cells, but not in dorsal root ganglia and PC12 neuronal cell lines. Furthermore, frataxin deficiency caused a significant increase in cell death uniquely in Schwann cells via the activation of inflammatory pathways. In consistent with the “dying back” hypothesis of FRDA, the inflammogens secreted by frataxin-deficient Schwann cells could be toxic to the axons of dorsal root ganglia with which they are in intimate contact *in vivo*, and eventually leads to the loss of DRG neurons. It is still unclear why frataxin deficiency activates the inflammatory pathways and leads to cell death selectively in Schwann cells, however these observations do provide a cellular basis for the selective demyelination and vulnerability of DRG neurons in FRDA.. Further *in vivo* investigations are needed to confirm these *in vitro* observations.

Acknowledgements

This work was supported by USPHS Grants AG11967, AG16719, EY12245 and AG23311. We thank Carol Oxford for technical assistance with the flow cytometer.

References

[1] J.T. Hughes, B. Brownell and R.L. Hewer, The peripheral sensory pathway in friedreich's ataxia. An examination by light and electron microscopy of the posterior nerve roots, posterior root ganglia, and peripheral sensory nerves in cases of friedreich's ataxia, Brain 91 (1968) 803-818.

[2] D. Oppenheimer and M. Esiri, Disease of the basal ganglia, cerebellum and motor neurons, 5 ed., Arnold, London, 1992.

[3] S. Al-Mahdawi, R.M. Pinto, D. Varshney, L. Lawrence, M.B. Lowrie, S. Hughes, Z. Webster, J. Blake, J.M. Cooper, R. King and M.A. Pook, GAA repeat expansion mutation mouse models of Friedreich ataxia exhibit oxidative stress leading to progressive neuronal and cardiac pathology, Genomics 88 (2006) 580-590.

[4] G. Said, M.H. Marion, J. Selva and C. Jamet, Hypotrophic and dying-back nerve fibers in Friedreich's ataxia, Neurology 36 (1986) 1292-1299.

[5] N. Rizzuto, S. Monaco, G. Moretto, S. Galiazzo-Rizzuto, A. Fiaschi, A. Forti and R. De Maria, Friedreich's ataxia. A light- and electron microscopic study of peripheral nerve biopsies, Acta Neuropathol Suppl 7 (1981) 344-347.

[6] J.G. McLeod, An electrophysiological and pathological study of peripheral nerves in Friedreich's ataxia, J Neurol Sci 12 (1971) 333-349.

[7] S. Jitpimolmard, J. Small, R.H. King, J. Geddes, P. Misra, J. McLaughlin, J.R. Muddle, M. Cole, A.E. Harding and P.K. Thomas, The sensory neuropathy of Friedreich's ataxia: an autopsy study of a case with prolonged survival, Acta Neuropathol 86 (1993) 29-35.

[8] A.E. Harding and R.L. Hewer, The heart disease of Friedreich's ataxia: a clinical and electrocardiographic study of 115 patients, with an analysis of serial electrocardiographic changes in 30 cases, Q J Med 52 (1983) 489-502.

[9] G. Finocchiaro, G. Baio, P. Micossi, G. Pozza and S. di Donato, Glucose metabolism alterations in Friedreich's ataxia, Neurology 38 (1988) 1292-1296.

[10] C. Lu and G. Cortopassi, Frataxin knockdown causes loss of cytoplasmic iron-sulfur cluster functions, redox alterations and induction of heme transcripts, Arch Biochem Biophys 457 (2007) 111-122.

[11] H. Puccio, D. Simon, M. Cossee, P. Criqui-Filipe, F. Tiziano, J. Melki, C. Hindelang, R. Matyas, P. Rustin and M. Koenig, Mouse models for Friedreich ataxia exhibit cardiomyopathy, sensory nerve defect and Fe-S enzyme deficiency followed by intramitochondrial iron deposits, Nat Genet 27 (2001) 181-186.

[12] M.M. Santos, K. Ohshima and M. Pandolfo, Frataxin deficiency enhances apoptosis in cells differentiating into neuroectoderm, Hum Mol Genet 10 (2001) 1935-1944.

[13] B. Bonetti, P. Valdo, C. Stegagno, R. Tanel, G.L. Zanusso, D. Ramarli, E. Fiorini, S. Turazzi, M. Carner and G. Moretto, Tumor necrosis factor alpha and human Schwann cells: signalling and phenotype modulation without cell death, J Neuropathol Exp Neurol 59 (2000) 74-84.

[14] R. Murwani, S. Hodgkinson and P. Armati, Tumor necrosis factor alpha and interleukin-6 mRNA expression in neonatal Lewis rat Schwann cells and a neonatal rat Schwann cell line following interferon gamma stimulation, J Neuroimmunol 71 (1996) 65-71.

[15] D.S. Skundric, R.P. Lisak, M. Rouhi, B.C. Kieseier, S. Jung and H.P. Hartung, Schwann cell-specific regulation of IL-1 and IL-1Ra during EAN: possible relevance for immune regulation at paranodal regions, J Neuroimmunol 116 (2001) 74-82.

[16] D.S. Skundric, B. Bealmear and R.P. Lisak, Induced upregulation of IL-1, IL-1RA and IL-1R type I gene expression by Schwann cells, J Neuroimmunol 74 (1997) 9-18.

[17] R. Wagner and R.R. Myers, Schwann cells produce tumor necrosis factor alpha: expression in injured and non-injured nerves, Neuroscience 73 (1996) 625-629.

[18] R.A. Schoenfeld, E. Napoli, A. Wong, S. Zhan, L. Reutenauer, D. Morin, A.R. Buckpitt, F. Taroni, B. Lonnerdal, M. Ristow, H. Puccio and G.A. Cortopassi, Frataxin deficiency alters heme pathway transcripts and decreases mitochondrial heme metabolites in mammalian cells, Hum Mol Genet 14 (2005) 3787-3799.

[19] J.W. Newman, T. Watanabe and B.D. Hammock, The simultaneous quantification of cytochrome P450 dependent linoleate and arachidonate metabolites in urine by HPLC-MS/MS, J Lipid Res 43 (2002) 1563-1578.

[20] G. Tan, E. Napoli, F. Taroni and G. Cortopassi, Decreased expression of genes involved in sulfur amino acid metabolism in frataxin-deficient cells, Hum Mol Genet 12 (2003) 1699-1711.

[21] G. Tan, L.S. Chen, B. Lonnerdal, C. Gellera, F.A. Taroni and G.A. Cortopassi, Frataxin expression rescues mitochondrial dysfunctions in FRDA cells, Hum Mol Genet 10 (2001) 2099-2107.

[22] K. Bergsteinsdottir, A. Kingston, R. Mirsky and K.R. Jessen, Rat Schwann cells produce interleukin-1, J Neuroimmunol 34 (1991) 15-23.

[23] R.P. Lisak, D. Skundric, B. Bealmear and S. Ragheb, The role of cytokines in Schwann cell damage, protection, and repair, J Infect Dis 176 Suppl 2 (1997) S173-179.

[24] R.B. Oliveira, E.P. Sampaio, F. Aarestrup, R.M. Teles, T.P. Silva, A.L. Oliveira, P.R. Antas and E.N. Sarno, Cytokines and Mycobacterium leprae induce apoptosis in human Schwann cells, J Neuropathol Exp Neurol 64 (2005) 882-890.

[25] G. Stoll, S. Jung, S. Jander, P. van der Meide and H.P. Hartung, Tumor necrosis factor-alpha in immune-mediated demyelination and Wallerian degeneration of the rat peripheral nervous system, J Neuroimmunol 45 (1993) 175-182.

[26] H. Akiyama, S. Barger, S. Barnum, B. Bradt, J. Bauer, G.M. Cole, N.R. Cooper, P. Eikelenboom, M. Emmerling, B.L. Fiebich, C.E. Finch, S. Frautschy, W.S. Griffin, H. Hampel, M. Hull, G. Landreth, L. Lue, R. Mrak, I.R. Mackenzie, P.L. McGeer, M.K. O'Banion, J. Pachter, G. Pasinetti, C. Plata-Salaman, J. Rogers, R. Rydel, Y. Shen, W. Streit, R. Strohmeyer, I. Tooyoma, F.L. Van Muiswinkel, R. Veerhuis, D. Walker, S. Webster, B. Wegrzyniak, G. Wenk and T. Wyss-Coray, Inflammation and Alzheimer's disease, Neurobiol Aging 21 (2000) 383-421.

[27] T. Wyss-Coray, Inflammation in Alzheimer disease: driving force, bystander or beneficial response?, Nat Med 12 (2006) 1005-1015.

[28] P.L. McGeer, K. Yasojima and E.G. McGeer, Inflammation in Parkinson's disease, Adv Neurol 86 (2001) 83-89.

[29] S.F. Crocker, W.J. Costain and H.A. Robertson, DNA microarray analysis of striatal gene expression in symptomatic transgenic Huntington's mice (R6/2) reveals neuroinflammation and insulin associations, Brain Res 1088 (2006) 176-186.

[30] E.M. Frohman, M.K. Racke and C.S. Raine, Multiple sclerosis--the plaque and its pathogenesis, N Engl J Med 354 (2006) 942-955.

[31] P. Weydt and T. Moller, Neuroinflammation in the pathogenesis of amyotrophic lateral sclerosis, Neuroreport 16 (2005) 527-531.

[32] G. Stoll, S. Jander and R.R. Myers, Degeneration and regeneration of the peripheral nervous system: from Augustus Waller's observations to neuroinflammation, J Peripher Nerv Syst 7 (2002) 13-27.

[33] O. Bourde, R. Kiefer, K.V. Toyka and H.P. Hartung, Quantification of interleukin-6 mRNA in wallerian degeneration by competitive reverse transcription polymerase chain reaction, J Neuroimmunol 69 (1996) 135-140.

[34] A.L. Constable, P.J. Armati, K.V. Toyka and H.P. Hartung, Production of prostanoids by Lewis rat Schwann cells in vitro, Brain Res 635 (1994) 75-80.

[35] A.L. Constable, P.J. Armati and H.P. Hartung, DMSO induction of the leukotriene LTC4 by Lewis rat Schwann cells, J Neurol Sci 162 (1999) 120-126.

[36] E.K. Mathey, J.D. Pollard and P.J. Armati, TNF alpha, IFN gamma and IL-2 mRNA expression in CIDP sural nerve biopsies, J Neurol Sci 163 (1999) 47-52.

[37] K.R. Bales, Y. Du, R.C. Dodel, G.M. Yan, E. Hamilton-Byrd and S.M. Paul, The NF-kappaB/Rel family of proteins mediates Abeta-induced neurotoxicity and glial activation, Brain Res Mol Brain Res 57 (1998) 63-72.

[38] L. Meda, M.A. Cassatella, G.I. Szendrei, L. Otvos, Jr., P. Baron, M. Villalba, D. Ferrari and F. Rossi, Activation of microglial cells by beta-amyloid protein and interferon-gamma, Nature 374 (1995) 647-650.

[39] J. Cohen, The immunopathogenesis of sepsis, Nature 420 (2002) 885-891.

[40] R.M. Adibhatla and J.F. Hatcher, Phospholipase A(2), reactive oxygen species, and lipid peroxidation in CNS pathologies, BMB Rep 41 (2008) 560-567.

[41] S. Michael, S.V. Petrocine, J. Qian, J.B. Lamarche, M.D. Knutson, M.D. Garrick and A.H. Koeppen, Iron and iron-responsive proteins in the cardiomyopathy of Friedreich's ataxia, Cerebellum 5 (2006) 257-267.

[42] D. Russell, Myocarditis in Friedreich's ataxia, J Path Bact 63 (1946) 739-748.

[43] M.R. Hejtmancik, J.Y. Bradfield, Jr. and G.V. Miller, Myocarditis and Friedreich's ataxia; a report of two cases, Am Heart J 38 (1949) 757-765, illust.

[44] G. Chodaczek, A. Saavedra-Molina, A. Bacsi, M.L. Kruzel, S. Sur and I. Boldogh, Iron-mediated dismutation of superoxide anion augments antigen-induced allergic inflammation: effect of lactoferrin, Postepy Hig Med Dosw (Online) 61 (2007) 268-276.

[45] L. Michalec, B.K. Choudhury, E. Postlethwait, J.S. Wild, R. Alam, M. Lett-Brown and S. Sur, CCL7 and CXCL10 orchestrate oxidative stress-induced neutrophilic lung inflammation, J Immunol 168 (2002) 846-852.

Tables

Table 1. Flow cytometry data of HOG and Schwann cells upon frataxin depletion at day 3.

	UR (dead)		LL (viable)		LR (early apoptotic)	
	ave	stv	ave	stv	ave	stv
HOG-scr	5.3	1.1	87.0	2.5	3.5	0.9
HOG-si	8.2	0.5	80.3	1.3	4.2	0.3
Sch-scr	5.4	0.1	88.6	0.1	5.1	0.7
Sch-siFxn	21.8	1.2	46.0	1.6	29.6	0.4
Sch-si-Q-VD	10.7	2.9	66.6	4.7	20.0	2.9

HOG-scr: scramble control in HOG cells, HOG-si: siFxn in HOG cells, Sch-scr: scramble control in Schwann cells, Sch-si: siFxn in Schwann cells, Sch-si-Q-VD: Q-VD-OPH treatment after frataxin depletion in Schwann cells. Numbers represent averages from 3 independent experiments

Table 2. The most affected biological processes in frataxin-depletion Schwann cells (*).

Bioprocesses	**genes**	**p-value**
Upregulated		
inflammatory response	27	<10-12
immune response	33	2.18E-10
cell-cell signaling	30	2.18E-10
chemotaxis	15	9.55E-10
apoptosis	27	1.18E-09
signal transduction	59	5.58E-09
regulation of apoptosis	15	2.26E-08
Downregulated		
cell cycle	56	<10-12
cell division	32	<10-12
mitosis	29	<10-12
spindle organization and biogenesis	7	<10-12
G2 phase of mitotic cell cycle	7	3.84E-11
DNA replication	33	4.47E-11
DNA replication initiation	10	8.17E-11

*The top 500 up-regulated and top 500 down-regulated genes were processed by the Onto-express program, and the output biological processes were ranked by corrected *p*-value and the gene number of each biological process. The table includes the biological processes shown on the top of the list.

Table 3. Sequences of primers used in quantitative RT-PCR for selected genes.

Adding mouse/rat gapdh

Gene name	Species	Primer name	Primer sequences
IL1B	Human	IL1B-F	5'-AAA CAG ATG AAG TGC TCC TTC CAG G-3'
		IL1B-R	5'-TGG AGA ACA CCA CTT GTT GCT CCA-3'
IL6	Human	IL6-F	5'-CAC TCA CCT CTT CAG AAC G-3'
		IL6-R	5'-ATT TGT GGT TGG GTC AGG G-3'
TNF	Human	TNF-F	5'-ACA AGC CTG TAG CCC ATG TT-3'
		TNF-R	5'-AAA GTA GAC CTG CCC AGA CT-3'
NFkB2	Human	NFkB2-F	5'-GGA GCA AGA GGC CAA AGA ACT-3'
		NFkB2-R	5'-TAC AGG CCG CTC AAT CTT CAT-3'
NFkB1	Human	NFkB1-F	5'-ATA GCA CTG GCA GCT TCA CAA-3'
		NFkB1-R	5'-CGA AGC TGG ACA AAC ACA GAG-3'
Fxn*	Mouse /rat	Fxn-F*	5'-GAT CAA CAA GCA GAC CCC AAA-3'
		Fxn -R*	5'-AGG CCA ATG AAG ACA AGT CCA-3'
FXN*	Human	FXN-F	5'-ACT AGC AGA GGA AAC GCT GG-3'
		FXN -R	5'-AGG CTT TAG TGA GCT CTG CG-3'
GAPDH	Human	GAPDH-F	5'-CCC CTG GCC AAG GTC ATC CAT G-3'
		GAPDH-R	5'-CAG TGA GCT TCC CGT TCA GCT C -3'
GAPDH	rat	GAPDH-F	5' TCA AGA AGG TGG TGA AGC AGG 3'
		GAPDH -R	5' GGT CTG GGA TGG AAT TGT GAG 3'

Fxn/FXN: Frataxin, Fxn-F/Fxn -R*: the forward and reverse primers are located in the consensus sequences of rat and mouse Frataxin gene.

Legends to Figures:

Fig.1. The effects of frataxin depletion by siRNA on proliferation and viability at day 3. A, Frataxin depletion by siRNA in human Schwann cell line T265 (Sch), human oligodendroglioma cell line (HOG) and Human neuronal cell line (NT2), rat neuronal cell line (PC12), rat/mouse DRG cell line (ND7/23) and rat DRG cell line (50B11). Frataxin mRNA levels were measured by quantitative PCR and represented as percentage of the basal expression in each cell line transfected with the scrambled siRNA (scr). B, frataxin depletion leads to significantly decreased viability uniquely in Schwann cells. C, Frataxin depletion causes about 5-fold increase in floating cells in frataxin-depleted Schwann cells. D, frataxin depletion causes proliferation inhibition in Schwann cells, HOG cells and NT2 cells, but not in PC12 and two DRG neuron lines. Error Bars represent averages ± standard deviations (n=3-8, $P<0.05$*, $P<0.01$**, $P<0.001$***).

Fig.2. Inhibition of cell proliferation and IL6 cytokine induction precede death in frataxin-deficient Schwann cells. The floating cells and the adherent cells in the same well were collected separately, and counted by trypan blue exclusion assay using the Beckman Coulter Vi-Cell cell counter. Total viable cell number was divided by total cell number from both parts to obtain the viability. Frataxin depletion results in a significant decrease in proliferation 1 day after siRNA transfection and becomes more severe at day 2 and day 3 (A). Frataxin depletion only causes significantly increased floating cells (B) and significantly decreased viability (C) at day 2, and both becomes more severe at day 3. IL6

levels are presented as fold change over the basal levels in scrambled controls (D). E, frataxin protein levels at day1, 2 and 3 upon siRNA transfection, shown here are representative western blotting data out of three independent experiments and bar graph from densitometry analysis of 3 independent experiments (frataxin protein levels were normalized to beta-actin levels). Bars represent averages ± standard deviations (n=3, P<0.05*, P<0.01**, P<0.001***).

Fig. 3. Frataxin deficiency leads to cell proliferation inhibition and cell cycle profile alteration in both Schwann and HOG cells. Quantification of cell-cycle distribution at day 3 and statistical analysis is presented in the bar graph. Bars represent averages ± standard deviations of three independent assay samples (n=3 P<0.05*, P<0.01**, P<0.001***).

Fig.4. Frataxin depletion causes a morphological change in T265 Schwann cells (Magnification, 20X). A, image of the scramble control of Schwann cells at day 3. B, image of frataxin-depleted Schwann cells at day 3.

Fig.5. Inflammatory and death transcripts are induced by frataxin deficiency in T265 Schwann cells by quantitative RT-PCR. Error Bars represent averages ± standard deviations (n=3 P<0.05*, P<0.01**, P<0.001***).

Fig.6. Cytokine protein levels are induced by frataxin deficiency in Schwann cells by multiplex ELISA assay. Cytokine levels are presented as fold change over the basal levels in scrambled controls. The average basal level (pg/ml/million cells) of each cytokine: IL6= 349.55, IL1a= 1.16, GCSF= 4.73, IL1b= 0.74, IL8= 5784, TNFa= 24.64, GMCSF= 92.27. Error Bars represent averages ± standard deviations (n=4, P<0.05*, P<0.01**, P<0.001***).

Fig.7. Inflammatory arachidonate metabolites increase in frataxin-deficient Schwann Cells. *(*A), A schematic of arachidonate pathway, (B and C),15 Inflammatory Lipoxygenase metabolites are increased significantly (with P value < 0.02) in frataxin-deficient Schwann Cells (if F-test was significant ($p < 0.05$, TTEST for two-sample unequal variance was applied, otherwise, TTEST for two-sample equal variance was applied).

Fig.8. Dexamethasone and SB203580 (a specific inhibitor of p38 MAP kinase) partially rescue cell death in frataxin-depleted Schwann cells. Dexamethasone (250nM) and SB203580 (20μM) treatment significantly decrease the floating cells in frataxin-depletion Schwann cells (A), Dexamethasone and SB203580 treatment significantly increase the viability in frataxin-depletion Schwann cells (B) Error Bars represent averages ± standard deviations (n=3 for dexamethasone treatment, n=4 for SB203580 treatment, P<0.05*, P<0.01**, P<0.001***).

Fig.9. The effect of Q-VD-OPH, Dexamethasone and SB203580 treatments on the cytokine protein expressions. Q-VD-OPH (5μM) does not decrease TNF and

IL6 protein levels at all, Dexamethasone significantly decrease IL6 and IL1A protein levels and decrease TNF protein levels non-significantly, SB203580 decreases IL1A protein levels significantly and decreases IL6 protein levels non-significantly. Error Bars represent averages ± standard deviations (n=3-8, P<0.05*, P<0.01**, P<0.001***).

Fig.10. Frataxin depletion results in an insignificant increase in mean phosphorylation of p38 MAP kinase at day 3. Western results of MAP kinase (P38, JNK and P42/44) in scrambled controls (SCR) and frataxin-depleted Schwann cells (siFxn) at 3 days post-knockdown (A). Bar graph represents the densitometry results of the western blots (B). Error Bars represent averages ± standard deviations (n=4). The difference in phosphorylation of p38 MAP kinase between scrambled controls (SCR) and frataxin-depleted Schwann cells (siFxn) is not significant.

Figures:

Fig.1

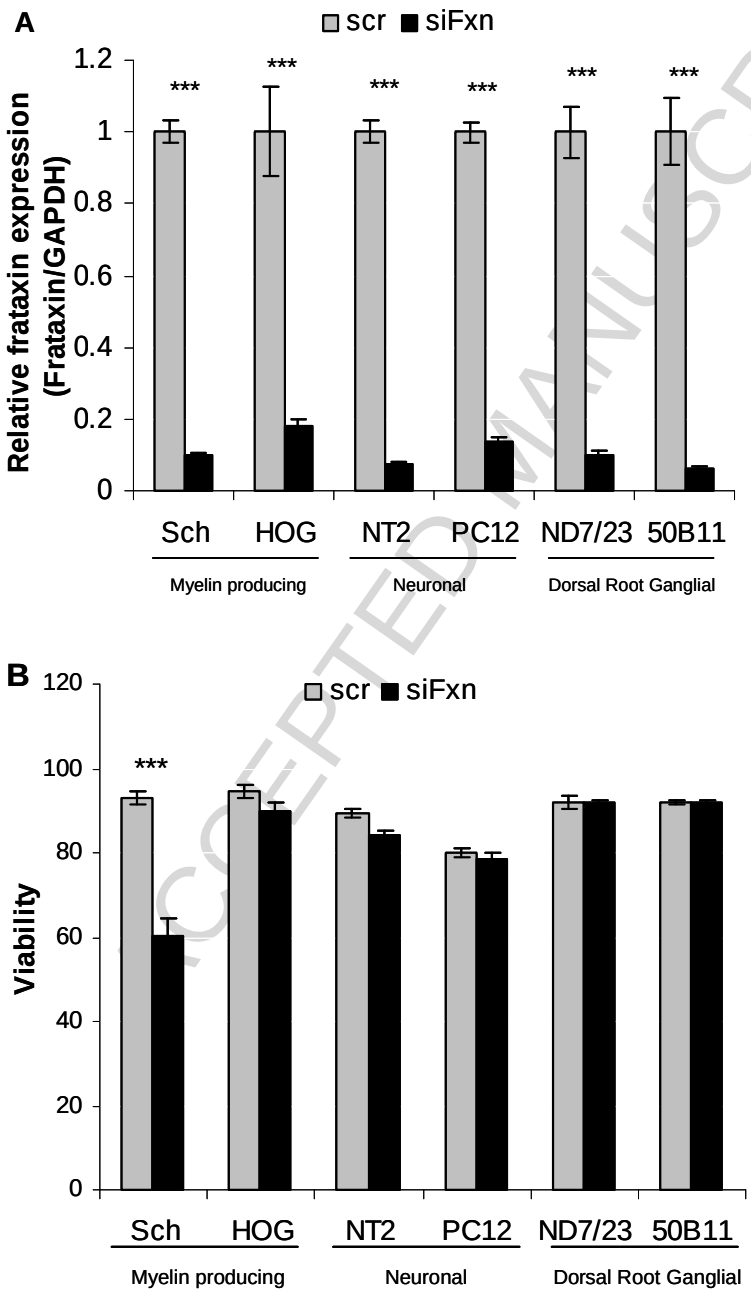

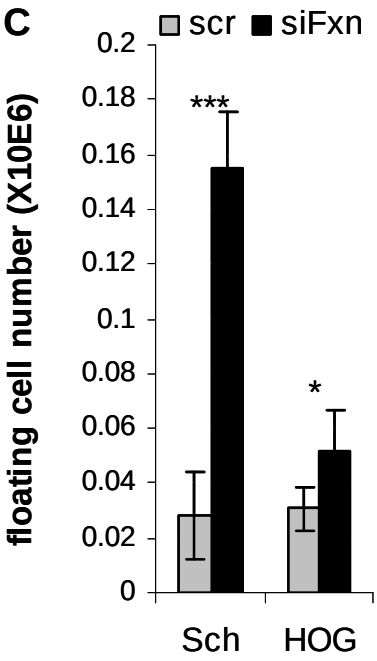

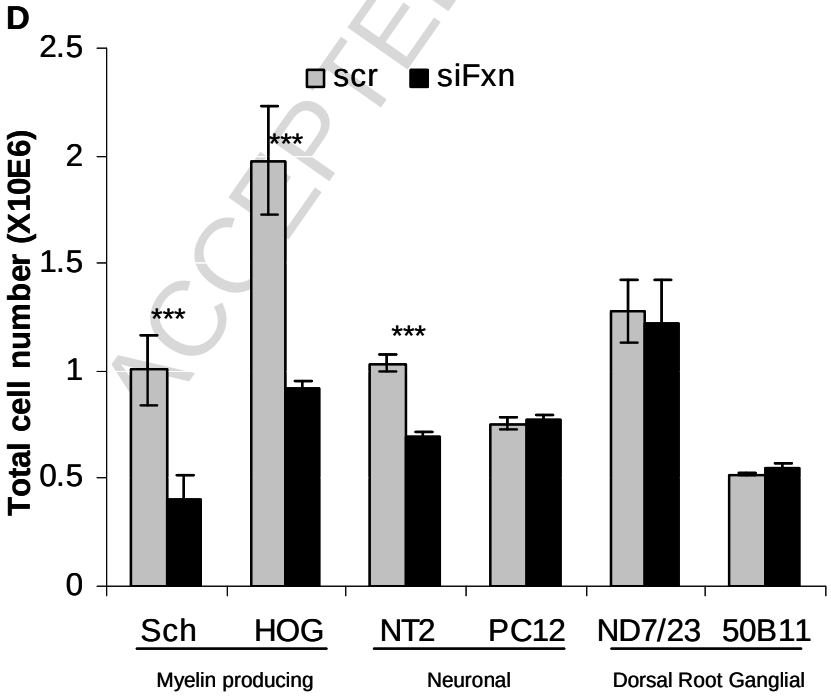

Fig.2

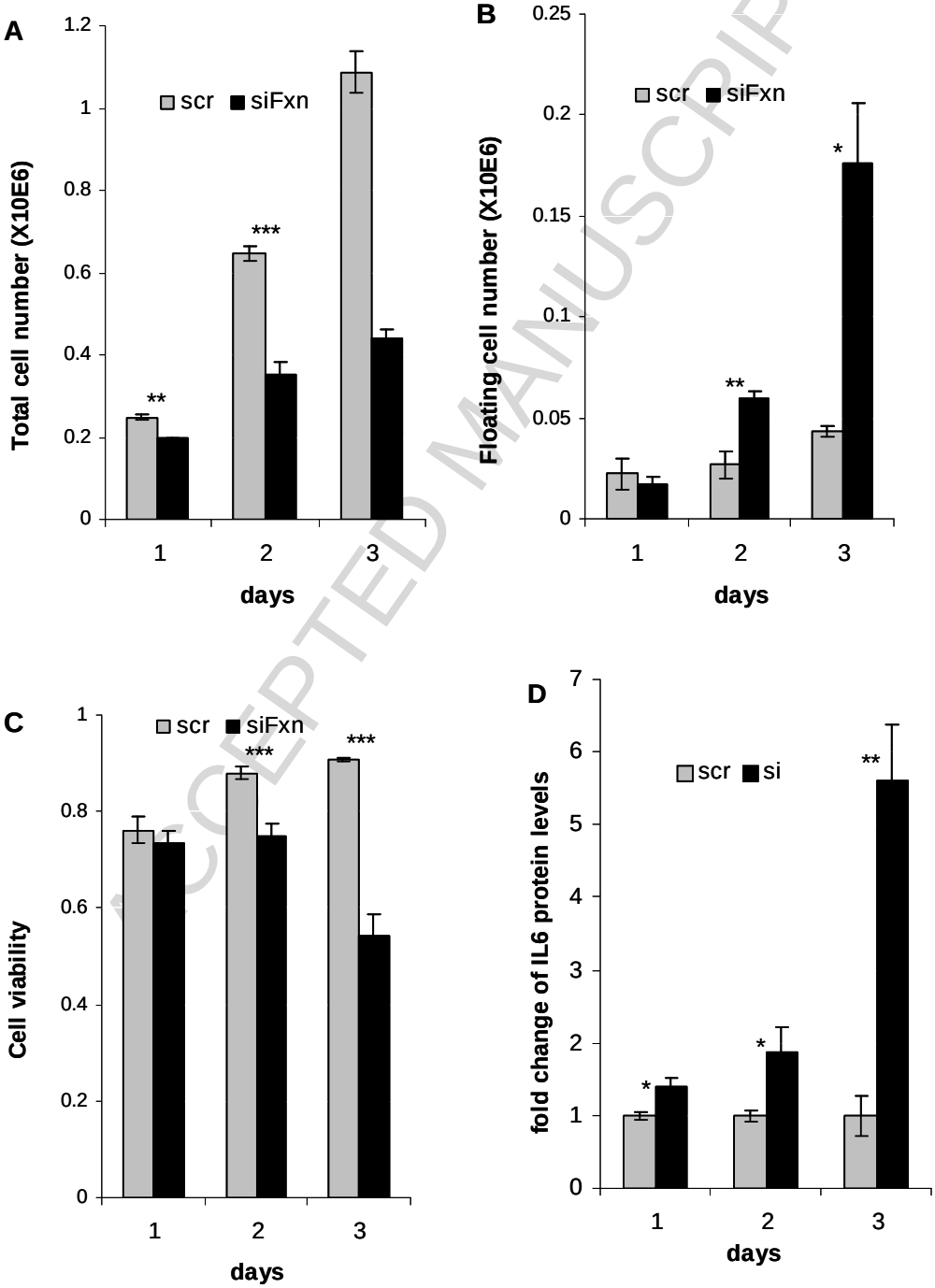

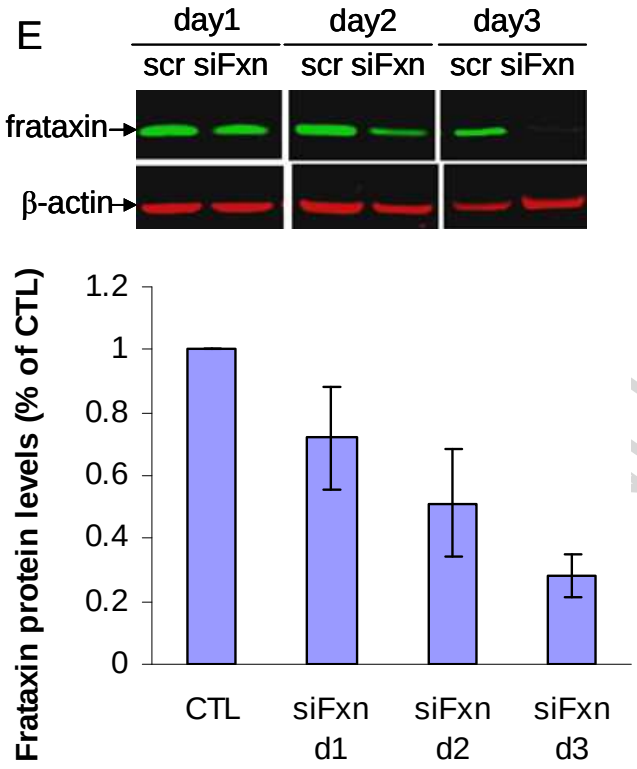

Fig.3

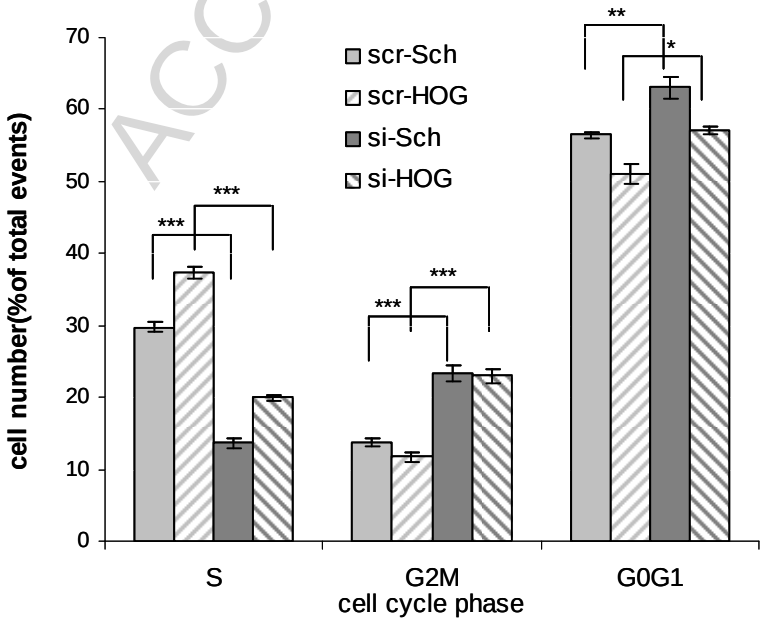

Fig.4

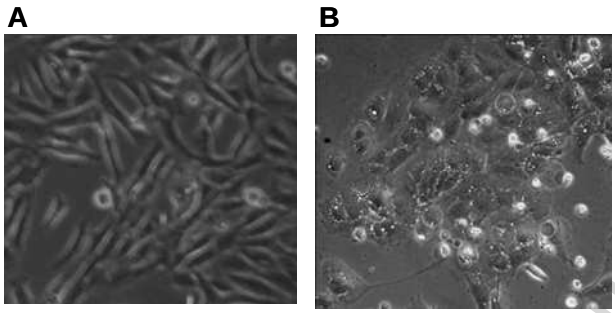

Fig.5

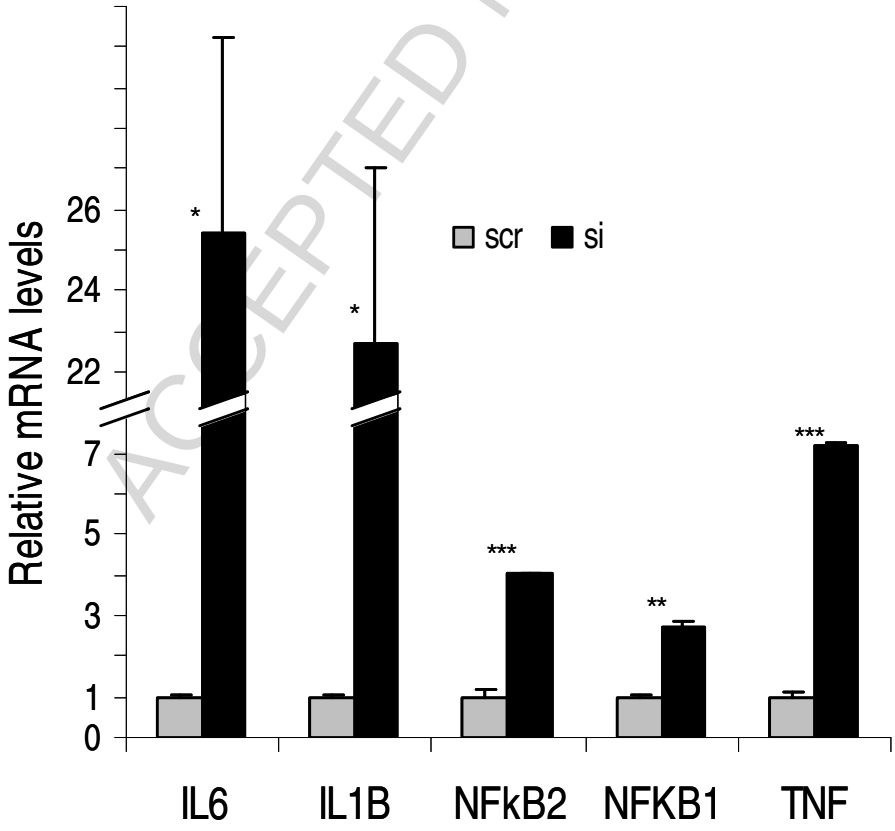

Fig.6

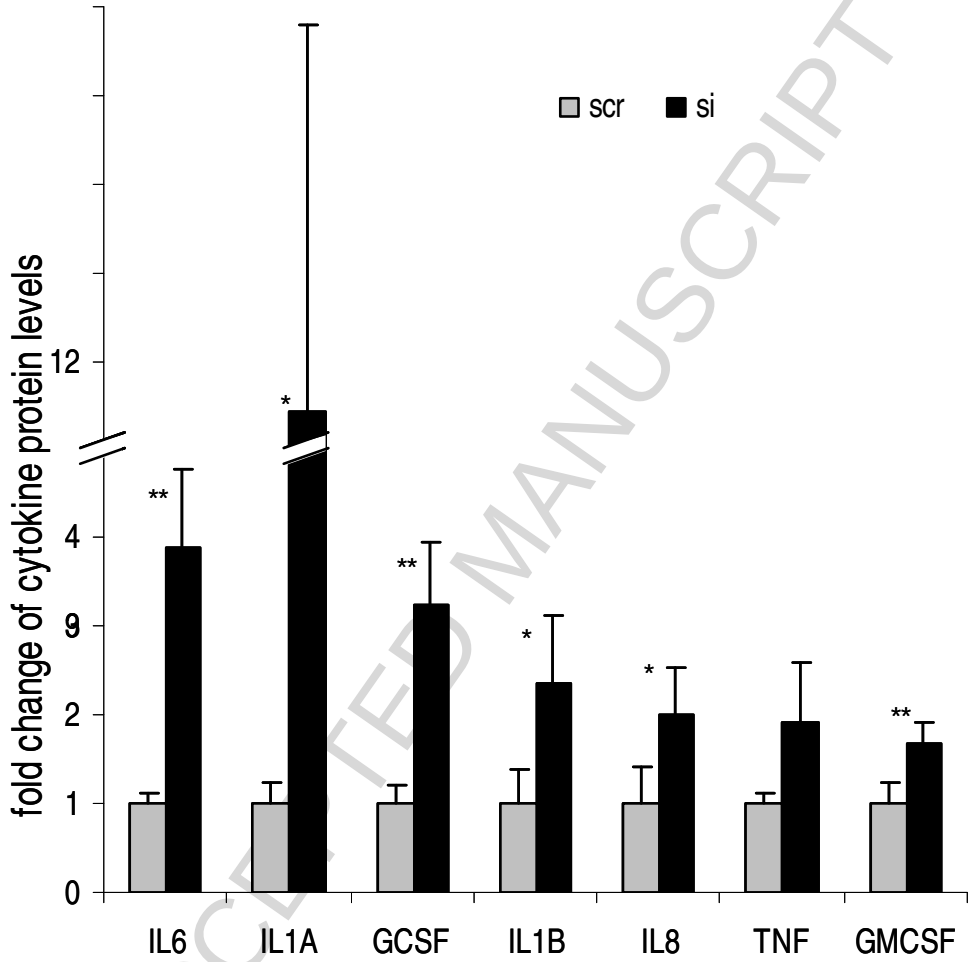

Fig.7

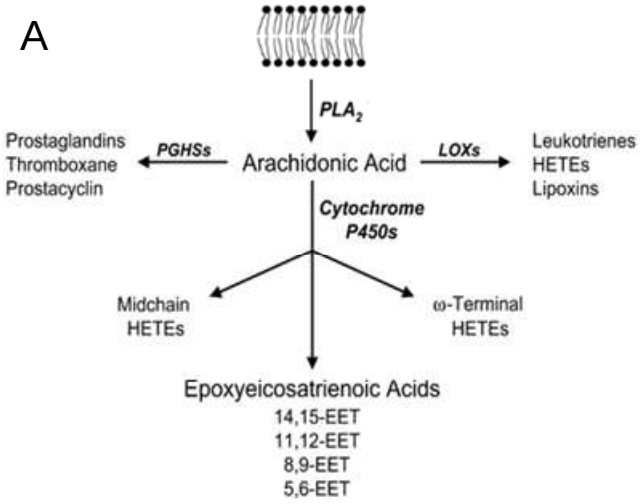

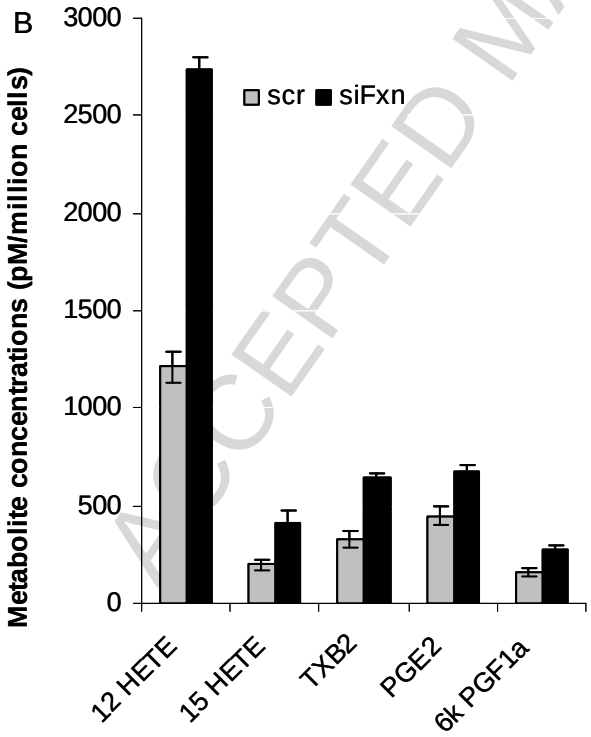

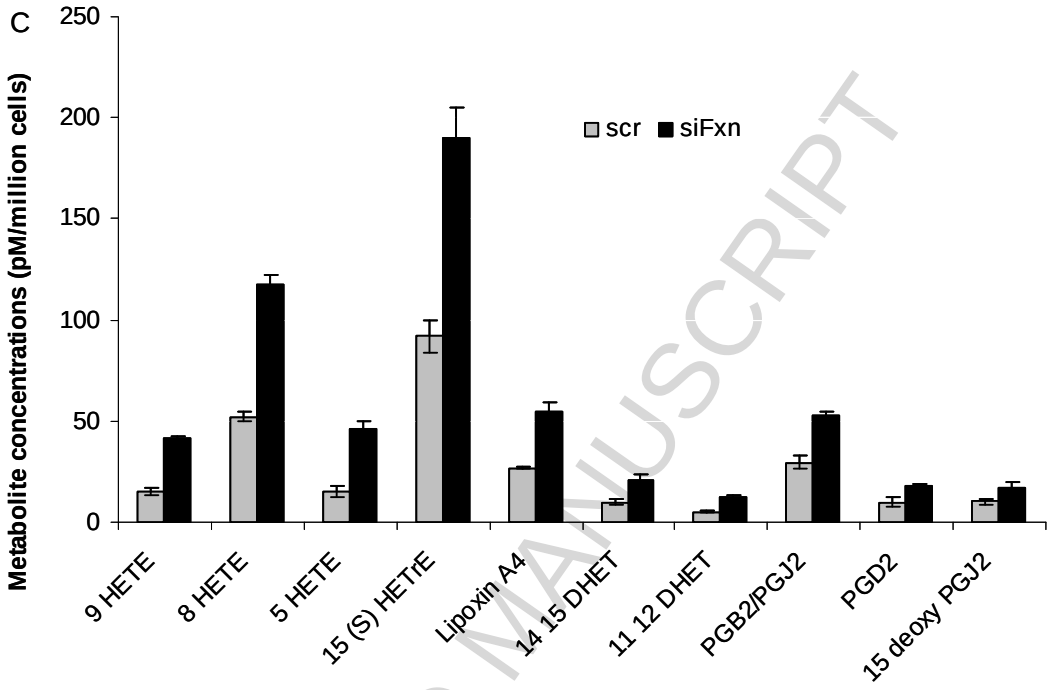

Fig.8

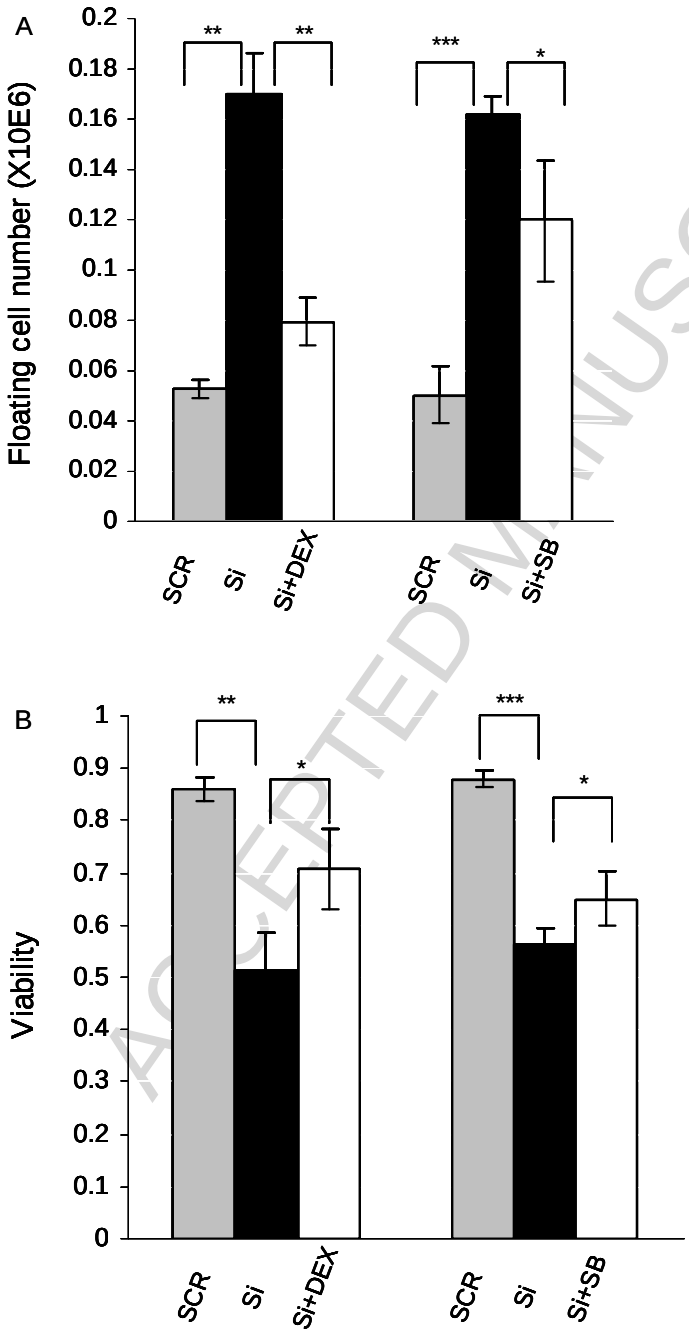

Fig. 9.

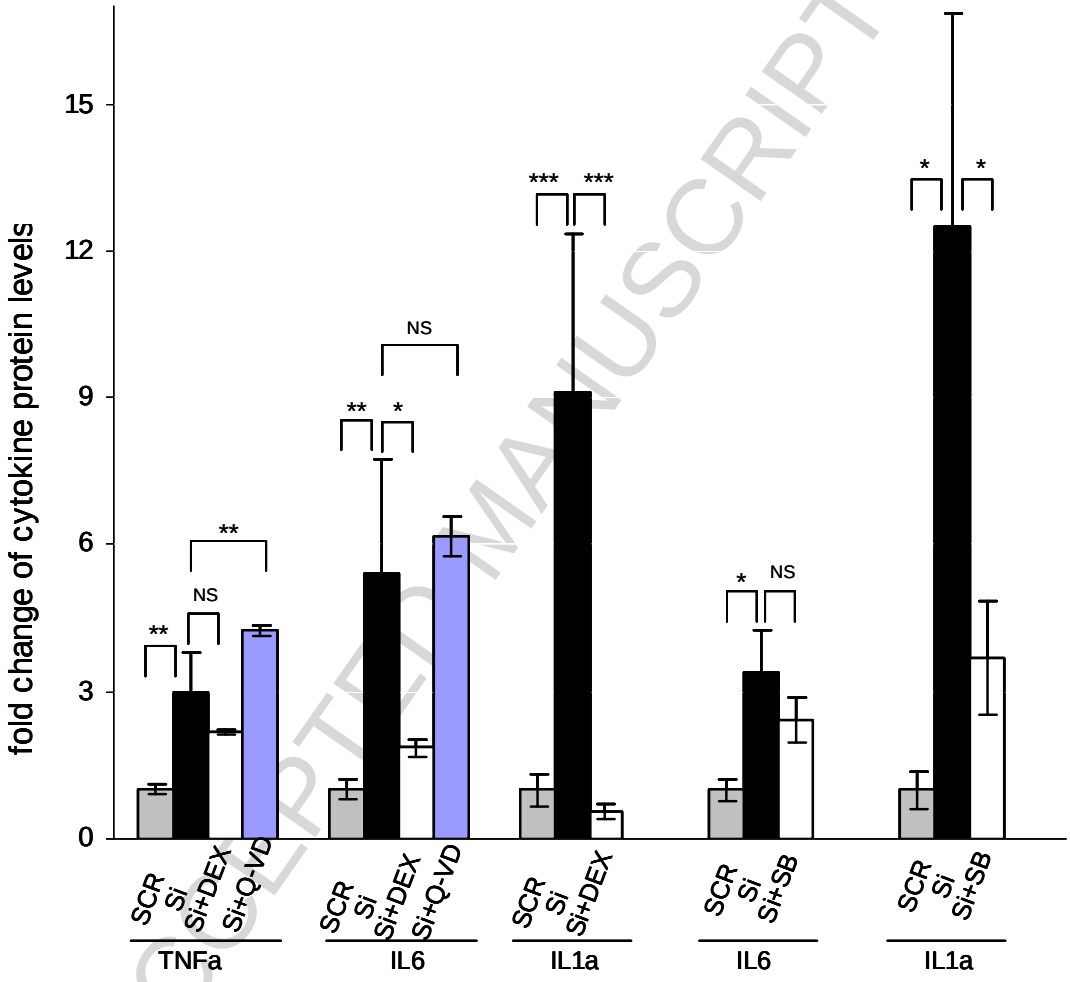

Fig.10